26th IEEE International Symposium on Personal, Indoor and Mobile Radio Communications (PIMRC), Hong Kong, Aug. 2015

DOI: 10.1109/PIMRC.2015.7343269

Static Sequence Assisted Out-of-Band Power Suppression for DFT-s-OFDM

F. Hasegawa
S. Shinjo
A. Okazaki
A. Okamura
L. Brunel
D. Mottier

Static Sequence Assisted Out-of-Band Power Suppression for DFT-s-OFDM

Fumihiro Hasegawa[†*], Shintaro Shinjo[†], Akihiro Okazaki[†] and Atsushi Okamura[†]
[†]Information Technology R&D Center, Mitsubishi Electric Corporation, 5-1-1 Ofuna, Kanagawa, Japan
Loïc Brunel[‡] and David Mottier[‡]
[‡] Mitsubishi Electric R&D Centre Europe, CS 10806, 35708 Rennes Cedex 7, France.
Email: *Hasegawa.Fumihiro@bk.MitsubishiElectric.co.jp

***Abstract*—A novel static sequence assisted discrete Fourier transform (DFT)-spread-orthogonal frequency division multiplexing (OFDM) waveform without cyclic prefix (CP) is proposed to suppress out-of-band (OoB) emission. A measure of continuity is proposed to determine the location of the static sequence to maximize the amount of OoB suppression. Furthermore, perturbation is added to the static sequence to improve phase continuity at block transitions. It is shown that the spectra of the proposed waveforms are more compact that those of the conventional waveforms. A frequency offset estimation method using the static sequence is described and its performance is evaluated by simulations.**

I. Introduction

DFT-spread-OFDM (DFT-s-OFDM) has been adopted in the uplink in Long Term Evolution (LTE) [1] thanks to its robust performance against multipath fading channels and low peak to average power ratio (PAPR). However, due to phase discontinuity at block transitions, out-of-band (OoB) emission becomes a concern in OFDM-based transmissions. Windowing techniques can be used to lower OoB at the expense of reduced length of cyclic prefix (CP) [2].

We propose a novel DFT-s-OFDM transmission scheme to suppress OoB emission in this paper. The proposed waveform does not contain CP but maintains robustness against multipath fading channels as well as low PAPR. Four contributions are presented in this paper. Firstly, similar to [3], a measure of continuity is derived. However, it should be noted that the contributions in [3] deal with DFT-s-OFDM with CP. Secondly, CP-less DFT-s-OFDM aided by a static sequence is proposed to lower the OoB emission in DFT-s-OFDM. The location of the static sequence to maximize the OoB suppression performance is determined by the measure of continuity. Similarities between the proposed method and zero-tail DFT-s-OFDM [4] are also described in this paper. Thirdly, a novel method in which the aforementioned static sequence is perturbed to further lower OoB is proposed. Finally, a frequency offset estimation method is proposed and its performance with or without perturbation is evaluated.

Insertion of zeros in place of CP for OFDM after inverse discrete Fourier transform (IDFT) is addressed in numerous studies [5], [6]. Insertion of a pseudo noise sequence as CP for OFDM was proposed in [7]. However, since a sequence of zeros or pseudo noise sequence is inserted after IDFT in the aforementioned studies, phase discontinuity between OFDM blocks still remains. It should also be mentioned that the proposed measure of continuity can also be used to evaluate the suppression performance of zero-tail DFT-s-OFDM.

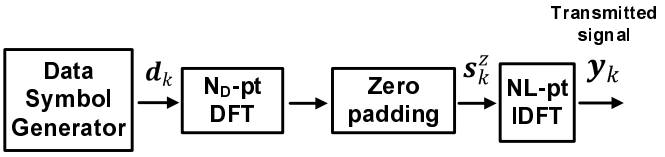

Fig. 1. DFT-s-OFDM transmitter without cyclic prefix

This paper is organized as follows. A signal model and proposed measure of continuity are introduced in Section II. The novel static sequence assisted DFT-s-OFDM is proposed and its average squared Euclidean distance (ASED) performance is evaluated in Section III. A novel perturbation based OoB suppression method is introduced in Section IV. A frequency offset estimation method using the proposed static sequence is described in Section V. Performance comparisons between the proposed and conventional methods are shown in Section VI and concluding remarks are included in Section VII.

II. Signal model and measure of continuity

A. Block format and conventional transmitter

The signal model and proposed measure of continuity are introduced in this section. Let us denote N_D and N as the number of data symbols and number of carriers in a DFT-s-OFDM block, respectively. First, assuming even N_D and N, discrete Fourier transform (DFT) precoded symbols are generated by $s_{k,n} = \frac{1}{\sqrt{N_D}} \sum_{m=0}^{N_D-1} e^{-j2\pi mn/N_D} d_{k,m}$, where $-N_D/2 \leq n \leq N_D/2 - 1$ and N_D data symbols for the k^{th} block are expressed as $\mathbf{d}_k = [d_{k,0}, \cdots, d_{k,N_D-1}]^T$. It is assumed that $E_S = E\left[|d_{k,i}|^2\right] = 1$ and $E\left[d_{k,m} d_{l,n}^*\right] = 0$ if $k \neq l$ or $m \neq n$. Then, the precoded symbols are mapped onto N_D carriers with $(N - N_D)/2$ zeros on each side as a guard band. Finally, N carriers are converted to time-domain signals by IDFT. The DFT-s-OFDM transmitter without a CP generator is shown in Fig.1.

Let us define a column vector which contains N zeros and $N \times N$ DFT matrix as $\mathbf{0}_N$ and $\mathbf{W}_N$, respectively, where the $(m,n)^{th}$ element of $\mathbf{W}_N$ is given by

$[\mathbf{W}_N]_{m,n} = e^{-j2\pi mn/N}/\sqrt{N}$. Then, the precoded symbols, padded with zeros for oversampling, can be written as $\mathbf{s}_z = \left[s_{k,0}, \cdots, s_{k,N_D/2-1}, \mathbf{0}^T_{LN-N_D}, s_{k,-N_D/2}, \cdots, s_{k,-1}\right]^T$ [8], where L denotes the oversampling rate. The output of the IDFT corresponding to the k^{th} block, which contains LN samples, is written as $\mathbf{y}_k = [y_{k,0}, \cdots, y_{k,LN-1}]^T = \mathbf{W}^H_{LN}\mathbf{s}^z_k$. The last LN_{CP} samples of $\mathbf{y}_k$, denoted as $\mathbf{y}_{CP,k} = \left[y_{k,L(N-N_{CP})}, \cdots, y_{k,NL-1}\right]^T$, are used as CP in the conventional DFT-s-OFDM [1], where N_{CP} denotes the number of samples in CP. The transmitted signal with CP can be written as $\mathbf{y}'_k = [\mathbf{y}^T_{CP,k}, \mathbf{y}^T_k]^T$. Negative sample indices are used to express the samples from the previous block as follows, $y_{k-1,n} = y_{k,n-LN}$.

B. Proposed measure of continuity

Similar to [3], let us now present a measure of continuity which is used to evaluate the OoB power suppression performance of the proposed method. As explained in [9], OoB power suppression for OFDM can be achieved by setting derivatives of the signal continuous at block transitions. Thus, denoting T_S as the duration of a block interval, OoB power suppression for DFT-s-OFDM without CP can be achieved by setting derivatives of the signal continuous at block transitions as follows, $\frac{d^n}{dt^n}x_k(t)|_{t=0} = \frac{d^n}{dt^n}x_{k-1}(t)|_{t=T_S}$, where $x_k(t)$ denotes DFT-s-OFDM signal for the k^{th} block without CP. Using the analog representation of the OFDM signal [9] [10], an analog representation of a DFT-s-OFDM waveform for the k^{th} block can be written as $x_k(t) = \frac{1}{\sqrt{T_S}}\sum_{l=-\frac{N_D}{2}}^{\frac{N_D}{2}-1} s_{k,l}e^{j2\pi l\frac{t}{T_S}}$, where $x_k(t)$ is assumed to be nonzero for $0 \le t < T_S$ and $x_k(t) = 0$ elsewhere. Substitution of $s_{k,l}$ into $x_k(t)$ gives us the following analog representation of the DFT-s-OFDM waveform, $x_k(t) = c\sum_{m=0}^{N_D-1} d_{k,m}\sum_{l=-N_D/2}^{N_D/2-1} e^{-j2\pi l\left(\frac{m}{N_D}-\frac{t}{T_S}\right)}$, where $c = \frac{1}{\sqrt{N_D T_S}}$. It can be shown that the p^{th} derivative of $x_k(t)$, denoted as $x_k^{(p)}(t)$, is written as $x_k^{(p)}(t) = \sum_{m=0}^{N_D-1} d_{k,m}\alpha_m^{(p)}(t)$, where $\alpha_m^{(p)}(t)$ is defined as $\alpha_m^{(p)}(t) = c\left(\frac{j2\pi}{T_S}\right)^p\sum_{l=-N_D/2}^{N_D/2-1} l^p e^{-j2\pi l\left(\frac{m}{N_D}-\frac{t}{T_S}\right)}$. Let us introduce $\alpha_m^{(p)} = \alpha_m^{(p)}(T_S) = \alpha_m^{(p)}(0)$ and following relationship

$$\alpha_m^{(p)} = c\left(\frac{j2\pi}{T_S}\right)^p \sum_{l=-N_D/2}^{N_D/2-1} l^p e^{\frac{-j2\pi lm}{N_D}}. \tag{1}$$

Let us also define a term which is used as a measure of continuity in this paper, $\varepsilon^{(p)} = x_k^{(p)}(0) - x_{k-1}^{(p)}(T_S)$. The term in $\varepsilon^{(p)}$ indicates continuity between blocks at the p^{th} derivative. By substituting $x_k^{(p)}(t)$ and (1) in $\varepsilon^{(p)}$, $\varepsilon^{(p)}$ can be rewritten as

$$\varepsilon^{(p)} = \sum_{m=0}^{N_D-1} \alpha_m^{(p)}\beta_m, \tag{2}$$

where β_m is defined as $\beta_m = d_{k,m} - d_{k-1,m}$. It can be shown that ASED at block transitions $E\left[\left|\varepsilon^{(p)}\right|^2\right]$ can be expressed as follows,

$$E\left[\left|\varepsilon^{(p)}\right|^2\right] = 2\sum_{m=0}^{N_D-1}\left|\alpha_m^{(p)}\right|^2. \tag{3}$$

It should be noted that ASED in (3) does not depend on the data symbols. In addition, unlike the method in [3], there is no constraint on N and N_D due to the absence of CP in the proposed method.

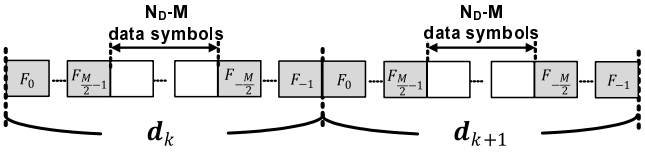

Fig. 2. Proposed placement of a static sequence

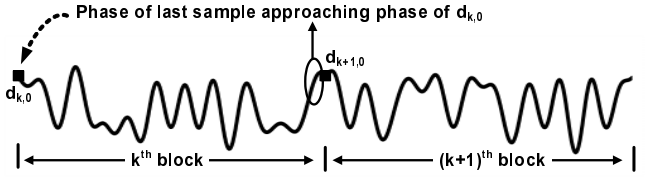

Fig. 3. Zeroth-order continuity, $d_{k+1,0} = d_{k,0}$

III. Proposed static sequence

A. Proposed placement

Similar to the method in [4], the goal here is to create cyclicity at consecutive block transitions to improve continuity between blocks. Let us define a static sequence as $\left[\mathbf{F}_1^T, \mathbf{F}_0^T\right]$, where $\mathbf{F}_1 = \left[F_{-M/2}, F_{-M/2+1}, \cdots, F_{-1}\right]^T$ and $\mathbf{F}_0 = \left[F_0, F_1, \cdots, F_{M/2-1}\right]^T$. Then, the static sequence can be placed as follows:

$$\begin{aligned} d_{k+1,n-1} &= d_{k,n-1} = F_{n-1} \\ d_{k+1,N_D-n} &= d_{k,N_D-n} = F_{-n} \end{aligned} \tag{4}$$

for $1 \le n \le M/2$ when $M \le N_D$. As the result of the presence of the static sequence, the number of data symbols in the proposed scheme is $N_D - M$. In the proposed scheme, the parameter M controls the amount of OoB power suppression. For clarity, the proposed sequence placement is shown in Fig. 2. From Fig. 2, it is obvious that cyclicity is created at consecutive block transitions. It should be mentioned here that setting $d_{k+1,0} = d_{k,0} = F_0$ satisfies the 0^{th} order continuity. An illustrative example of the 0^{th} order continuity when $d_{k+1,0} = d_{k,0}$ is shown in Fig. 3. Thanks to periodicity in the IDFT output [8], $x_k(T_S)$ approaches $d_{k,0}$ which is also the first sample of the next block $x_{k+1}(0) = c \cdot N_D \cdot d_{k,0}$. It is also clear from (1) and (2) that satisfying $d_{k+1,0} = d_{k,0}$ achieves the 0^{th} order continuity $\varepsilon^{(0)} = 0$ since $\alpha_m^{(0)} = 0$ for $m \neq 0$, $\alpha_0^{(0)} = c \cdot N_D$ and $\beta_0 = 0$.

Note that when the static sequence in (4) is replaced by zeros such that $F_{n-1} = 0$ and $F_{-n} = 0$ for $1 \le n \le M/2$,

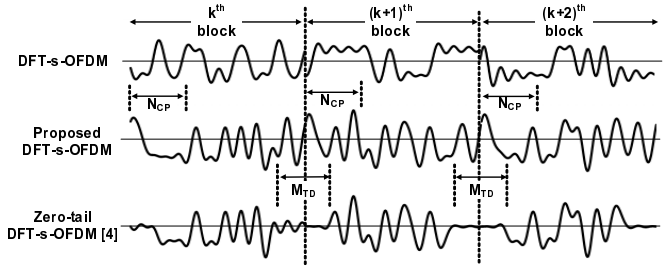

Fig. 4. Comparison of the waveforms generated by DFT-s-OFDM, zero-tail DFT-s-OFDM [4] and proposed method, $M = 8$ and $N_D = 24$, $N = 32$ for zero-tail DFT-s-OFDM and proposed method, $N = 22$, $N_D = 16$, $N_{CP} = 10$ for DFT-s-OFDM

the proposed method becomes the zero-tail DFT-s-OFDM [4]. A comparison of the waveforms generated by the conventional DFT-s-OFDM, zero-tail DFT-s-OFDM and proposed DFT-s-OFDM is shown in Fig. 4. The real part of $\mathbf{y}_k$ with quadrature phase shift keying (QPSK) is shown in the figure. From the figure, it is obvious that while phase discontinuity exists between blocks in the waveform generated by the conventional DFT-s-OFDM, the static or all-zero sequence guarantees phase continuity at block transitions. In the example, the following Zadoff-Chu sequence [11] is used as the static sequence in (4), $\left[F_0, \cdots, F_{M/2-1}, F_{-M/2}, \cdots, F_{-1}\right] = \left[1, \cdots, e^{\frac{-j\pi k^2}{M}}, \cdots, e^{\frac{-j\pi(M-1)^2}{M}}\right]$. As indicated in Fig. 4, the length of the static sequence at the output of the IDFT are defined as follows, $M_{TD} = \left\lfloor \frac{M \cdot N}{N_D} \right\rfloor$. As shown in Fig. 4, N and N_D are adjusted such that $M_{TD} \approx N_{CP}$. In addition, the parameters used to generate the waveforms in Fig. 4 are chosen in order to have the same block length and number of data symbols per block.

B. ASED performance analysis

Note from (2) that ASED in (3) can be reduced if the data symbols satisfy the following condition, $d_{k+1,m} = d_{k,m}$ for $m \in I_F$ where I_F is a set of symbol indices chosen from $\{0, 1, \cdots, N_D - 1\}$ and cardinality of I_F is given by $M = |I_F|$. For example, the proposed symbol placement in (4) can be expressed as $I_F = \{0, \cdots, M/2 - 1, N_D - M/2, \cdots, N_D - 1\}$. Furthermore, it can be shown that ASED is given by

$$E\left[\left|\varepsilon^{(p)}\right|^2\right] = 2 \sum_{m \notin I_F} \left|\alpha_m^{(p)}\right|^2. \tag{5}$$

By comparing (3) and (5), it is obvious that reduction in ASED by $2\sum_{m \in I_F} \left|\alpha_m^{(p)}\right|^2$ is achieved with the proposed method. It is also important to note from (3) that the ASED performances are independent of the choice of the static sequence and amount of ASED reduction depends on the location of the static sequence. In the following, let us investigate $\alpha_m^{(p)}$.

It is clear from (1) that $\alpha_m^{(p)}$ is the m^{th} coefficient of the DFT of l^p. In Fig. 5, normalized $\left|\alpha_m^{(p)}\right|^2$, which is defined as

TABLE I
PERFORMANCE IMPROVEMENT FACTOR δ WHEN $N_D = 1200$

p	1	2	3	4
$d_{k+1,0} = d_{k,0} = F_0$	-0.0	-3.5	0.00	-1.9
$M = 6$	-6.9	-22.5	-3.4	-14.4
$M = 80$	-18.2	-56.6	-14.5	-48.0

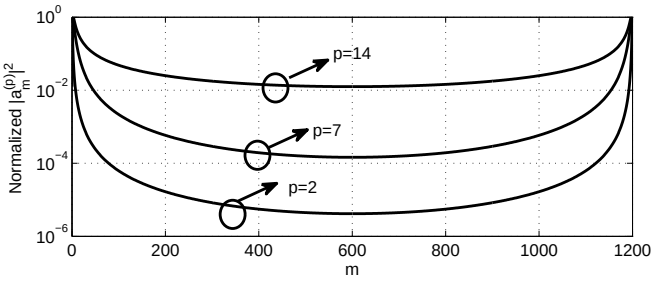

Fig. 5. Normalized $\left|\alpha_m^{(p)}\right|^2$, $N_D = 1200$

$\alpha_{\text{norm}}^{(p)} = \frac{\left|\alpha_m^{(p)}\right|^2}{\max_{0 \le n \le N_D - 1}\left(\left|\alpha_n^{(p)}\right|^2\right)}$, is shown for $p = \{2, 7, 14\}$. From the figure, it is clear that $\alpha_{\text{norm}}^{(p)}$ decreases as m approaches $N_D/2$. Moreover, it is notable from the figure that for smaller values of p, the energy of l^p is heavily concentrated around $m = 0$. As p increases the distribution of the energy of l^p spreads toward higher frequency. Thus, consecutive placement of the static symbols at both edges of a block (4) leads to more reduction in ASED $E\left[\left|\varepsilon^{(p)}\right|^2\right]$ for all values of p. Simply put, consecutive static symbols at both edges of the block introduce the static waveform at block transitions which lead to smoother phase transition.

Theoretical ASED performance of the proposed scheme (5) is shown in Table I. In the table, $d_{k+1,0} = d_{k,0} = F_0$ corresponds to the special case when only one symbol per block is static. The proposed method with $N_D = 1200$, which corresponds to one of the parameters specified in [12], is considered here. For each value of p, all ASED performances of the proposed methods are normalized by the ASED performance of DFT-s-OFDM without any OoB power suppression techniques as follows, $\delta = 10\log_{10}\left(\frac{\sum_{m \notin I_F}\left|\alpha_m^{(p)}\right|^2}{\sum_{m=0}^{N_D-1}\left|\alpha_m^{(p)}\right|^2}\right)$. It is notable from Table I that increasing M improves the ASED performance.

IV. PROPOSED STATIC SEQUENCE WITH PERTURBATION

A. Computation of perturbation in the proposed method

In this subsection, an adaptive OoB suppression method is proposed to further reduce OoB. Let us denote a set of indices Ω chosen from $\{0, 1, \cdots, N_D - 1\}$ with cardinality $|\Omega| = M$. The perturbation vector $\mathbf{w}_k = [w_{k,0}, \cdots, w_{k,M-1}]^T$ is added to the data symbols located at the aforementioned indices to improve signal continuity at block transitions, obtaining $\tilde{\mathbf{d}}_{k,\Omega} = \mathbf{d}_{k,\Omega} + \mathbf{w}_k$. Let us represent the $N \times N$ DFT matrix as a partitioned matrix $\mathbf{W}_N = \left[\mathbf{W}_{N,0}^T \mathbf{W}_{N,1}^T\right]^T$

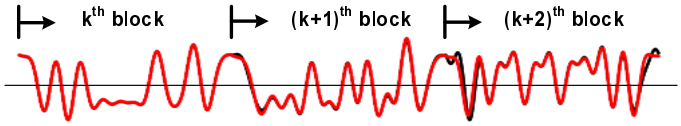

Fig. 6. Waveform of the proposed adaptive DFT-s-OFDM with or without perturbation, indicated by red and black solid line, respectively

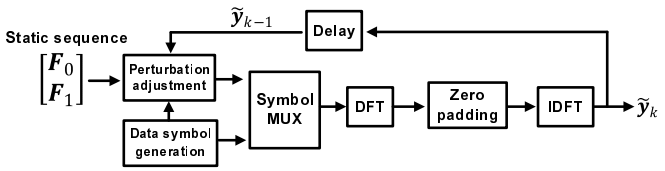

Fig. 7. Proposed transmitter with a perturbation generator

where $\mathbf{W}_{N,0}$ and $\mathbf{W}_{N,1}$ are both $N/2 \times N$ matrices. Then, let us define the following $NL \times N_D$ matrix $\mathbf{C} = \mathbf{W}_{NL}^H \left[\mathbf{W}_{N_D,0}^T, \mathbf{0}_{NL-N_D,N_D}^T, \mathbf{W}_{N_D,1}^T\right]^T$. Then, the output of IDFT corrupted by the perturbation vector can be written as $\tilde{\mathbf{y}}_k = \mathbf{y}_k + \mathbf{C}_\Omega \mathbf{w}_k$, where $\mathbf{C}_\Omega$ consists of the columns of $\mathbf{C}$ that correspond to the indices in Ω.

The perturbation vector is computed as follows. The goal is to compute $\mathbf{w}_k$ to minimize the Euclidian norm of the following samples at block transitions, $e_{k,n-1} = y_{k,NL-n} - \tilde{y}_{k-1,NL-n}$ and $e_{k,n+K/2-1} = y_{k,NL+n-1} - \tilde{y}_{k-1,n-1}$ for $1 \le n \le K/2$ where K indicates the number of oversamples. In this paper, perturbation is added to the static sequence described in the previous section, such that $\Omega = I_F$ where I_F is also defined in previous section. Denoting $\mathbf{C}_{S,\Omega}$ as a matrix that consists of the rows and columns that correspond to the indices $S = \{0, 1, \cdots, K/2-1, NL-K/2, \cdots, NL-1\}$ and Ω, respectively, the gap term $e_{k,n}$ can be expressed as $\mathbf{e}_k = [e_{k,0}, \cdots, e_{k,K-1}]^T = \mathbf{C}_{S,\Omega}\mathbf{w}_k$. The minimum norm solution [13] can be formulated as $\mathbf{w}_{k,\min} = \arg\min_{\mathbf{w}_k} |\mathbf{w}_k|^2$ such that $\mathbf{e}_k = \mathbf{C}_{S,\Omega}\mathbf{w}_k$. Assuming $K < M$, the minimum Euclidean norm solution for the above problem can be computed as $\mathbf{w}_k = \mathbf{C}_{S,\Omega}^H \left(\mathbf{C}_{S,\Omega} \cdot \mathbf{C}_{S,\Omega}^H\right)^{-1} \mathbf{e}_k$, where $\mathbf{C}^H$ is the Hermitian transpose of $\mathbf{C}$ with $\mathbf{w}_0 = \mathbf{0}_{M,1}$. Finally, adjustment to the static symbols is made as follows, $d_{k,m-1} = F_{m-1} + w_{k,M/2+m-1}$ and $d_{k,N_D-m} = F_{-m} + w_{k,M/2-m}$ for $1 \le m \le M/2$. The waveform with or without perturbation is shown in Fig. 6. It is clear from the figure that the addition of perturbation improves phase continuity at block transitions. A block diagram of the proposed transmitter is shown in Fig. 7.

B. ECP-OFDM [14]

In this subsection, ECP-OFDM proposed in [14] is briefly described. Let us denote a zero-padded vector of data symbols as $\mathbf{d}_k^z = \left[d_{k,0}, \cdots, d_{k,\frac{N_D}{2}-1}, \mathbf{0}_{LN-N_D}^T, d_{k,\frac{N_D}{2}}, \cdots, d_{k,N_D-1}\right]^T$, Then an OFDM waveform for the k^{th} block can be expressed as $\mathbf{y}_k = [y_{k,0}, \cdots, y_{k,NL-1}]^T = \mathbf{W}_{NL}^H \mathbf{d}_k^z$. The perturbation vector $\mathbf{w}_k = [w_{k,0}, \cdots, w_{k,NL-1}]^T$ is added to the OFDM waveform to obtain $\tilde{\mathbf{y}}_k = [\tilde{y}_{k,0}, \cdots, \tilde{y}_{k,NL-1}]^T = \mathbf{y}_k + \mathbf{w}_k$. Let us also represent rows between $(N - N_{CP})^{th}$ and $(N - N_{CP} + K - 1)^{th}$ row of $\mathbf{W}$ as $\tilde{\mathbf{W}}$ and define $e_{k,m} = \tilde{y}_{k-1,m} - y_{k,m+(N-N_{CP})L}$ for $m = 0, \cdots, K-1$. Following [14], perturbation is added to N_D data symbols. The perturbation vector is computed to minimize the average power of $\mathbf{f}_k = [f_{k,0}, \cdots, f_{k,N_D-1}]^T$ where $\mathbf{e}_k = [e_{k,0}, \cdots, e_{k,K-1}]^T = \tilde{\mathbf{W}}\mathbf{f}_k$. Then, the OFDM waveform with the perturbation vector can be expressed as $\tilde{\mathbf{y}}_k = \mathbf{y}_k + \mathbf{W}\tilde{\mathbf{W}}^H \left(\tilde{\mathbf{W}}\tilde{\mathbf{W}}^H\right)^{-1} \mathbf{e}_k$. It should be noted while only static symbols are perturbed in the proposed method, all data symbols are corrupted by perturbation in ECP-OFDM.

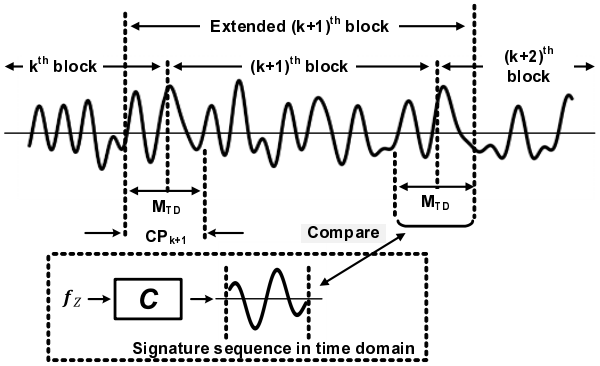

Fig. 8. Synchronization using the proposed static sequence

V. Proposed Frequency Synchronization Method

In this section, the proposed frequency offset estimation method is described. Thanks to insertion of the static sequence prior to the DFT, the proposed receiver can exploit the extended block in the proposed signal waveform which overlaps with adjacent extended blocks. Moreover, due to cyclicity, the static portion of in the waveform at the output of IDFT can be used as CP. The extended block and CP are illustrated in Fig. 8. It should be noted that the channel estimation based synchronization method cannot be implemented with the zero-tail DFT-s-OFDM [4], since the extended CP consists of zeros.

Let us describe the frequency offset estimation method using the static sequence. Assuming $L = 1$, the received signal model for the k^{th} block corrupted by both multi-path fading and frequency offset can be written as $r_{k,n} = e^{j2\pi\Omega n} \sum_{l=0}^{N_P-1} h_l y_{k,n-l} + n_{k,n}$ where M, n_k, h_l and Ω denote number of paths, additive white Gaussian noise (AWGN), fading coefficient and normalized frequency offset, respectively. The variance of AWGN is given by $\sigma_w^2 = E\left[|n_{k,n}|^2\right]$. Static fading channels are assumed in this paper. The frequency offset is estimated using the static sequence as follows. Let us express the static sequence in a DFT-s-OFDM block as $\mathbf{f}_Z = \left[\mathbf{F}_0^T, \mathbf{0}_{N_D-M}^T, \mathbf{F}_1^T\right]^T$. Using the partitioned representation of the Then the static sequence $\mathbf{f}_Z$ at the output of IDFT can be written as $\mathbf{f} = [f_0, f_1, \cdots, f_{N-1}]^T = \mathbf{C}\mathbf{f}_Z$ with $L = 1$ Finally, by extracting the extended CP shown in Fig. 8

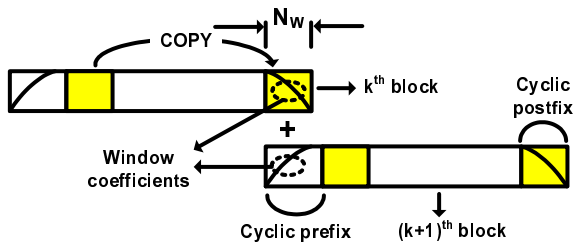

Fig. 9. Time windowing using cyclic prefix and postfix

from $\mathbf{f}$, we obtain the following signature sequence in the time domain, $\mathbf{p} = \left[p_{-\frac{M_{TD}}{2}}, p_{-\frac{M_{TD}}{2}+1}, \cdots, p_{\frac{M_{TD}}{2}-1}\right]^T = \left[f_{N-\frac{M_{TD}}{2}}, \cdots, f_{N-1}, f_0, \cdots, f_{\frac{M_{TD}}{2}-1}\right]^T$, where M_{TD} is assumed to be an even number. The above sequence is used to estimate the frequency offset in this section. The operation is illustrated in Fig. 8. In this paper, the frequency offset is estimated by testing several pre-defined offset candidate values. Using the channel estimation based technique [15] to estimate the offset, received signal after removal of the frequency offset based on the l^{th} candidate of the offset $\hat{\Omega}^{(l)}$ is given by $r_{k,n}^{(l)} = r_{k,n}e^{-j2\pi\hat{\Omega}^{(l)}n}$. Let us define the following $M_{TD} \times N_P$ matrix which consists $\mathbf{p}$,

$$\mathbf{B} = \begin{bmatrix} p_{-M_{TD}/2+N_P-1} & \cdots & p_{-M_{TD}/2} \\ p_{-M_{TD}/2+N_P} & \cdots & p_{-M_{TD}/2+1} \\ \vdots & \ddots & \vdots \\ p_{M_{TD}/2-1} & \cdots & p_{M_{TD}/2-N_P} \end{bmatrix}. \quad (6)$$

where $M_{TD} \geq 2N_P$. Using the notation introduced in Section II-A, a vector of the received signals which contains the signature sequence can be expressed as $\mathbf{r}_k = [r_{k,-M_{TD}/2+N_P}, r_{k,-M_{TD}/2+N_P+1}, \cdots, r_{k,M_{TD}/2-1}]^T$. Then, following channel estimate can be obtained, $\hat{\mathbf{h}}^{(l)} = \left(\mathbf{B}^H\mathbf{B}\right)^{-1}\mathbf{B}^H\mathbf{D}^{(l)}\mathbf{r}_k$, where $\mathbf{D}^{(l)} = \text{diag}\{1, e^{-j2\pi\hat{\Omega}^{(l)}}, \cdots, e^{-j2\pi\hat{\Omega}^{(l)}(M_{TD}-1)}\}$. Finally, the following metric is calculated $e^{(l)} = \left|\mathbf{r}_k - \mathbf{B}\hat{\mathbf{h}}^{(l)}\right|^2$, and the frequency offset candidate with the smallest metric is chosen as $l^* = \arg\min_l e^{(l)}$. It should be noted that slight degradation in the synchronization performance is expected when the perturbation based method described in Section IV is implemented, since the receiver assumes an undistorted static sequence (6).

VI. Simulation Results

Simulation results are shown in this section. In all simulations, QPSK modulation is implemented. As performance benchmarks, OFDM and DFT-s-OFDM without any OoB suppression techniques, and ECP-OFDM [14] are incorporated in the performance comparison. A windowing OoB suppression method for DFT-s-OFDM with a raised cosine window is also included in the comparison. The time windowing operation, as shown in Fig. 9, can be expressed as follows, $y'_{k+1,-N_{CP}L+n} = y_{k+1,-N_{CP}L+n} \cdot v_{0,n} + y_{k,n} \cdot v_{1,n}$ where

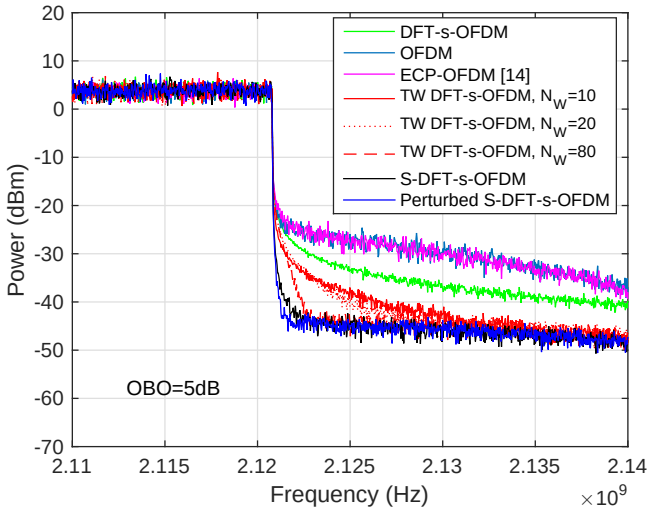

Fig. 10. Spectra of the proposed and conventional methods with an amplifier

$v_{0,n} = \frac{1}{2}\left(1 + \cos\left(\frac{n\pi}{N_W}\right)\right)$ and $v_{1,n} = \frac{1}{2}\left(1 - \cos\left(\frac{n\pi}{N_W}\right)\right)$ for $n = 0, \cdots, N_W - 1$. In Fig. 10, spectra of the conventional and proposed methods in the presence of an amplifier are shown. The signal bandwidth of 22MHz and center frequency of 2.11GHz are assumed in the simulation. In the figure, DFT-s-OFDM with time windowing, the proposed static-sequence assisted DFT-s-OFDM and perturbation-based method are labeled as "TW DFT-s-OFDM", "S-DFT-s-OFDM" and "Perturbed S-DFT-s-OFDM", respectively. The parameters used in the simulation are $N = 2048$, $N_D = 1200$, $M = 84$ and $K = 6$. For DFT-s-OFDM, OFDM and ECP-OFDM, $N = 2048$, $N_D = 1200$ and $N_{CP} = 144$ are used. It should be noted that $M_{TD} = \left\lfloor 84 \cdot \frac{2048}{1200} \right\rfloor - 1 = 142$ so that $M_{TD} \approx N_{CP}$. In the simulation, a hard limiter [16] is assumed as the amplifier and phase distortion due to amplification is assumed to be negligible. An output backoff value of OBO=5 dB is assumed in the simulation. Note that with time windowing, the effective CP length is reduced by $\frac{N_W}{L}$. For example, when $N_W = 80$, the effective CP length becomes $N'_{CP} = 144 - \frac{N_W}{L} = 144 - 20 = 124$. From Fig. 10, it is clear that spectra of the proposed S-DFT-s-OFDM waveforms are more compact those of the conventional methods and OoB suppression performance of ECP-OFDM deteriorates due to high PAPR of the OFDM waveform. In Fig. 11, adjacent channel leakage ratio (ACLR) performance of the proposed and conventional methods are shown. It is assumed that the adjacent signal is located 22MHz away from the center frequency. It is clear from Fig. 11 that the perturbed S-DFT-s-OFDM lowers ACLR compared to the conventional methods. In addition, S-DFT-s-OFDM yields the similar performance compared to the time windowing methods at lower values of output backoff values.

Effect of perturbation on peak power performance of DFT-s-OFDM is also investigated. The complementary cumulative distribution function (CCDF) of instantaneous normalized

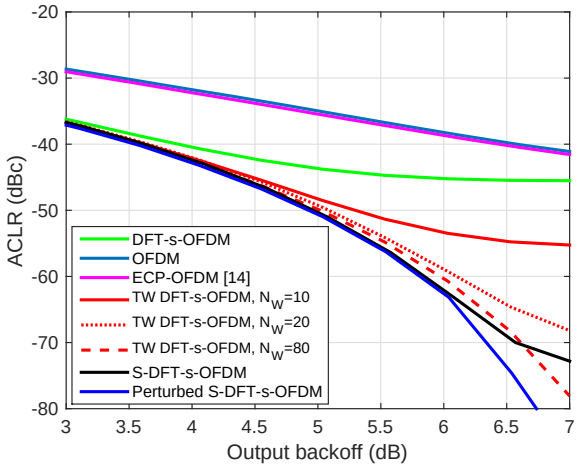

Fig. 11. ACLR performance comparison

TABLE II
INP PERFORMANCE COMPARISON: CCDF (INP(δ)) VERSUS δ IN DB

CCDF (INP(δ))	10^{-2}	10^{-3}	10^{-4}
DFT-s-OFDM	4.44	5.73	6.59
Perturbed S-DFT-s-OFDM	4.46	5.75	6.6

power (INP) [17], which is defined as $\text{CCDF}\left(\text{INP}(\delta)\right) = P\left(\frac{|y_{k,n}|^2}{E\left[|y_{k,n}|^2\right]} > \delta\right)$, with $L = 4$ is investigated. In the proposed perturbation method, $K = 8$ is implemented. The INP performances of DFT-s-OFDM and perturbed S-DFT-s-OFDM are shown in Table II. In the table, the threshold value δ to obtain $\text{CCDF}\left(\text{INP}(\delta)\right)$ is shown. From the table, it is clear that the addition of perturbation to the static sequence does not have significant impact on the INP performance of the proposed waveform.

In Table III, frequency offset estimation performance is shown. Estimation performance is evaluated by the mean square error (MSE) which is defined as $\text{MSE} = E\left[\left|\hat{\Omega} - \Omega\right|^2\right]$. In the simulation, $N_P = 11$ is assumed in the multipath channel model. In the proposed method, $K = 8$ is implemented and $e^{(m)}$ is averaged over three DFT-s-OFDM blocks for each frequency offset candidate. The signal to noise ratio (SNR) per bit is defined as $\frac{E_b}{\sigma_w^2} = \frac{E_S}{\sigma_w^2}\left(\frac{N}{N_D - M}\right)\left(\frac{1}{\log_2 X}\right)$, respectively, where $X = 2$ is used for QPSK. In the simulation, the frequency offset Ω is chosen randomly from the interval $[0, 0.01]$. In the synchronization algorithm, a frequency offset candidate $\hat{\Omega}^{(m)}$ is chosen from linearly-spaced candidates separated by $2.5 \cdot 10^{-4}$ in the interval $[0, 0.01]$. From Table III, it is clear that the addition of the perturbation vector causes slight degradation in frequency offset estimation performance.

VII. Conclusion

Novel OoB power suppression methods are proposed in this paper. The spectrum analysis and simulated ACLR results

TABLE III
FREQUENCY OFFSET ESTIMATION PERFORMANCE

SNR per bit (dB)	-5	0	5
S-DFT-s-OFDM	$2.24 \cdot 10^{-6}$	$3.99 \cdot 10^{-7}$	$6.02 \cdot 10^{-8}$
Perturbed S-DFT-s-OFDM	$2.06 \cdot 10^{-6}$	$4.15 \cdot 10^{-7}$	$6.23 \cdot 10^{-8}$

demonstrate that the proposed methods lower OoB emission compared to the conventional methods even in the presence of an amplifier. It is shown that the proposed static sequence can be used for frequency offset estimation. It is also observed that perturbation in the static sequence has negligible effects on the INP and frequency offset estimation performances.

VIII. Acknowledgment

The authors would also like to thank Dr. T. Nakakawaji and Mr. N. Yamada of Mitsubishi Electric Corporation for their encouragement and support throughout this work.

References

[1] H. Myung, J. Lim, and D. Goodman, "Single carrier FDMA for uplink wireless transmission," *IEEE Veh. Technol. Mag.*, vol. 1, no. 3, pp. 30–38, Sept. 2006.
[2] M. Faulkner, "The effect of filtering on the performance of OFDM systems," *IEEE Trans. Veh. Technol.*, vol. 49, no. 5, pp. 1877–1884, Sept. 2000.
[3] F. Hasegawa, A. Okazaki, A. Okamura, L. Brunel, and D. Mottier, "Novel dynamic and static methods for out-of-band power suppression in SC-OFDM," *IEEE Wireless Commun. Letters*, IEEE Early Access Articles 2015.
[4] G. Berardinelli, F. M. L. Tavares, T. B. Sørensen, P. Morgensen, and K. Pajukoski, "Zero-tail DFT-spread-OFDM signals," in *2013 IEEE Globecom Workshops*, Dec. 2013, pp. 229–234.
[5] S. Ohno, "Performance of single-carrier block transmissions over multipath fading channels with linear equalization," *IEEE Trans. on Signal Processing*, vol. 54, no. 10, pp. 3678–3687, Oct. 2006.
[6] J. Wang, J. Song, and L. Yang, "A novel equalization scheme for ZP-OFDM system over deep fading channels," *IEEE Trans. on Broadcasting*, vol. 56, no. 2, pp. 249–252, June 2010.
[7] J. Song, Z. Yang, L. Yang, K. Gong, C. Pan, J. Wang, and Y. Wu, "Technical review on Chinese digital terrestrial television broadcasting standard and measurements on some working modes," *IEEE Trans. on Broadcasting*, vol. 53, no. 1, pp. 1–7, March 2007.
[8] B. Porat, *A Course in Digital Signal Processing*. New York, NY, USA: John Wiley & Sons, 1997.
[9] J. van de Beek and F. Berggren, "N-continuous OFDM," *IEEE Commun. Lett.*, vol. 13, no. 1, pp. 1–3, Jan. 2009.
[10] X. Cai and G. B. Giannakis, "Bounding performance and suppressing intercarrier interference in wireless mobile OFDM," *IEEE Trans. on Commun.*, vol. 51, no. 12, pp. 2047–2056, Dec. 2003.
[11] D. Chu, "Polyphase codes with good periodic correlation properties," *IEEE Trans. Inf. Theory*, vol. 18, no. 4, pp. 531–532, Jul. 1972.
[12] "User equipment (UE) radio transmission and reception (release 12)," *3GPP TS 36.101 version 12.5.0*, Nov. 2014.
[13] J. van de Beek and F. Berggren, "Out-of-band power suppression in OFDM," *IEEE Commun. Lett.*, vol. 12, no. 9, pp. 609–611, Sept. 2008.
[14] Y. Jiang and Y. Wang, "A new out-of-band power suppression scheme by extending effective cyclic-prefix of OFDM," in *Proc. VTC 2010*, May 2010, pp. 1–5.
[15] Y. Wang, K. Shi, and E. Serpedin, "Continuous-mode frame synchronization for frequency-selective channels," *IEEE Trans. on Veh. Tech.*, vol. 53, no. 3, pp. 865–871, May 2004.
[16] "Digital video broadcasting (DVB); DVB-S2 extensions (DVB-S2X)," *ETSI EN 302 307 V1.1.1*, Oct. 2014.
[17] C. Ciochina, F. Buda, and H. Sari, "An analysis of OFDM peak power reduction techniques for WiMAX systems," in *Proc. ICC 2006*, vol. 10, 2006, pp. 4676–4681.